Article

Current Biology

Osmolality as a Novel Mechanism Explaining Diet Effects on the Outcome of Infection with a Blood Parasite

Graphical Abstract

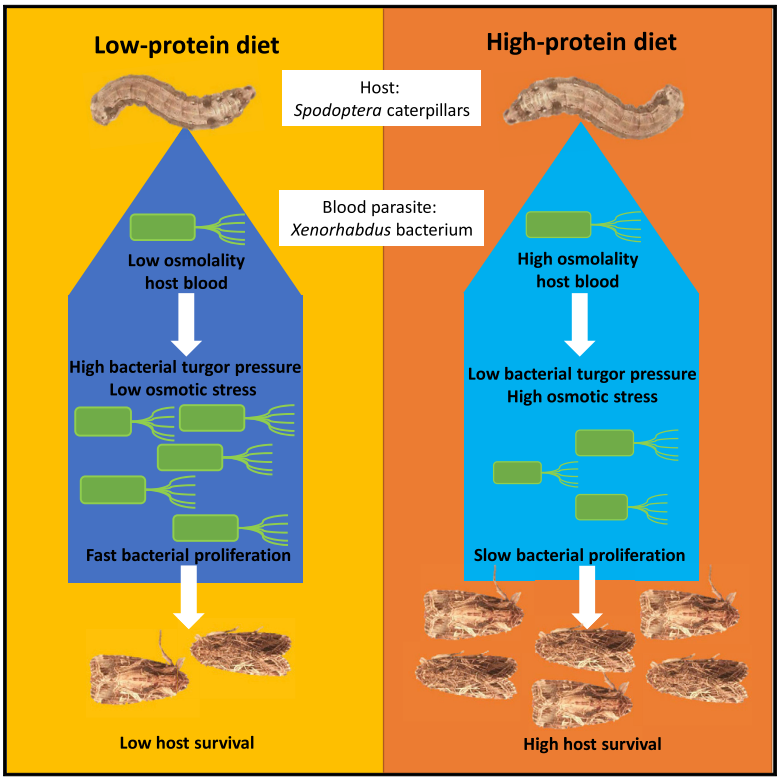

Highlights

- Outcome of infection with bacterial blood parasite is determined by dietary protein
- Dietary protein strongly limits bacterial establishment and growth in its host
- As dietary protein increases, so too does host blood osmolality (solute concentration)
- Bacterial proliferation declines as blood osmolality increases *in vivo* and *in vitro*

Authors

Kenneth Wilson, Robert Holdbrook, Catherine E. Reavey, ..., Stephen J. Simpson, Judith A. Smith, Sheena C. Cotter

Correspondence

ken.wilson@lancaster.ac.uk

In Brief

Diet can impact the ability to overcome infections. Here, Wilson et al. show that caterpillars are more likely to survive bacterial blood infections on high-protein diets because bacteria grow more slowly. *In vivo* and *in vitro* experiments indicate that this is because blood osmolality (solute concentration) increases, constraining bacterial growth.

Wilson et al., 2020, Current Biology *30*, 1–9
July 6, 2020
https://doi.org/10.1016/j.cub.2020.04.058

CellPress

Current Biology

CellPress
OPEN ACCESS

Article

Osmolality as a Novel Mechanism Explaining Diet Effects on the Outcome of Infection with a Blood Parasite

Kenneth Wilson,[1,6,7,*] Robert Holdbrook,[1] Catherine E. Reavey,[1] Joanna L. Randall,[1] Yamini Tummala,[1] Fleur Ponton,[2,3] Stephen J. Simpson,[2] Judith A. Smith,[4] and Sheena C. Cotter[5]

[1]Lancaster Environment Centre, Lancaster University, Lancaster LA1 4YQ, UK
[2]Charles Perkins Centre, The University of Sydney, Sydney, NSW 2006, Australia
[3]Department of Biological Sciences, Macquarie University, Sydney, NSW 2109, Australia
[4]School of Forensic and Applied Sciences, University of Central Lancashire, Preston, Lancashire PR1 2HE, UK
[5]School of Life Sciences, University of Lincoln, Brayford Pool, Lincoln LN6 7TS, UK
[6]Twitter: @spodoptera007
[7]Lead Contact
*Correspondence: ken.wilson@lancaster.ac.uk
https://doi.org/10.1016/j.cub.2020.04.058

SUMMARY

Recent research has suggested that the outcome of host-parasite interactions is dependent on the diet of the host, but most previous studies have focused on "top-down" mechanisms, i.e., how the host's diet improves the host immune response to drive down the parasite population and improve host fitness. In contrast, the *direct* impacts of host nutrition on parasite fitness and the mechanisms underpinning these effects are relatively unexplored. Here, using a model host-pathogen system (*Spodoptera littoralis* caterpillars and *Xenorhabdus nematophila*, an extracellular bacterial blood parasite), we explore the effects of host dietary macronutrient balance on pathogen growth rates both *in vivo* and *in vitro*, allowing us to compare pathogen growth rates both in the presence and absence of the host immune response. *In vivo*, high dietary protein resulted in lower rates of bacterial establishment, slower bacterial growth, higher host survival, and slower speed of host death; in contrast, the energy content and amount of carbohydrate in the diet explained little variation in any measure of pathogen or host fitness. *In vitro*, we show that these effects are largely driven by the impact of host dietary protein on host hemolymph (blood) osmolality (i.e., its concentration of solutes), with bacterial growth being slower in protein-rich, high-osmolality hemolymphs, highlighting a novel "bottom-up" mechanism by which host diet can impact both pathogen and host fitness.

INTRODUCTION

Nutrition is increasingly being seen as a key driver of the outcome of host-parasite interactions [1–4]. The mechanisms by which diet influences host-parasite interactions are still poorly understood and most of the literature in this area has tended to focus on the effects of key nutrients on host immune function [2, 5–11], i.e., "top-down" effects of nutrition on parasite fitness mediated by the host immune system [12]. An alternative or complementary scenario is that parasites are regulated by "bottom-up" effects, including the direct effects of specific nutrients on parasite proliferation [12]. Despite some evidence that both top-down and bottom-up processes could be important in determining the outcome of infections [12–16], there is a paucity of studies addressing the mechanisms of the bottom-up, diet-mediated control of parasite growth.

The literature regarding the importance of macronutrients in modulating immune defense and determining the outcome of host-pathogen interactions currently provides a mixed picture. There is evidence for energy [17], carbohydrate [9, 11, 18, 19], protein [6, 7, 20–22], lipid [23, 24], and/or their ratios [5, 8, 10, 25–27] all having a role to play in responses to parasitism. In most of these studies, it is difficult to interpret which specific dietary attribute is driving changes in immune function or survival following infection due to covariation in nutritional traits. Disentangling these relationships requires experimental designs that carefully decouple the various covarying nutritional traits.

Here, we apply the geometric framework for nutrition (GFN) to unravel the effects of macronutrient balance and calorie intake on the outcome of infection, using as a model host-pathogen system *Spodoptera littoralis* (a generalist leaf-feeding caterpillar) and *Xenorhabdus nematophila* (an extracellular gram-negative bacterium). In the wild, *X. nematophila* has a mutualistic association with the entomopathogenic nematode *Steinernema carpocapsae*, which serves to vector *X. nematophila* into insect hosts, entering them via orifices such as the mouth and spiracles, or penetrating through the insect cuticle, when they encounter potential hosts on the soil surface or on host plants [28, 29]. The bacterium is, however, also capable of killing insects without its nematode host when *X. nematophila* cells are injected directly into the insect hemocoel (the primary body cavity containing circulatory fluid) [29], so providing a tractable laboratory system for studying

Please cite this article in press as: Wilson et al., Osmolality as a Novel Mechanism Explaining Diet Effects on the Outcome of Infection with a Blood Parasite, Current Biology (2020), https://doi.org/10.1016/j.cub.2020.04.058

Table 1. Nutritional Composition of the Six Chemically Defined Diets and Model Explanatory Terms

Model	Diet	Protein (g/100-g diet)		Carbs (g/100-g diet)	Cal (kJ/100-g diet)		Perc (%)	P:C	Cellulose (g/100-g diet)
	A	2.8		14.0	326		17	1: 5	79.2
	B	8.4		8.4	326		50	1: 1	79.2
	C	14.0		2.8	326		83	5: 1	79.2
	D	10.5		52.5	1,112		17	1: 5	33.0
	E	31.5		31.5	1,112		50	1: 1	33.0
	F	52.5		10.5	1,112		83	5: 1	33.0
0. Null	–	–		–	–		–	–	–
1. Diet	X	–		–	–		–	–	–
2. Protein	–	X		–	–		–	–	–
3. Carb	–	–		X	–		–	–	–
4. P + C	–	X		X	–		–	–	–
5. P*C	–	X	*	X	–		–	–	–
6. Cal	–	–		–	X		–	–	–
7. Perc	–	–		–	–		X	–	–
8. Cal + Perc	–	–		–	X		X	–	–
9. Cal*Perc	–	–		–	X	*	X	–	–

Asterisks indicate interactions between terms (e.g., model 5 includes the interaction between protein and carbohydrate). P:C, ratio of soluble protein to digestible carbohydrate (P:C = 1:5, 1:1, or 5:1). Perc, relative percentage of protein in the digestible component of the diet (17%, 50%, or 83%); the remainder is carbohydrate. Cal, energy value of digestible nutrients in the diet (326 or 1,112 kJ/100-g diet), the remainder being non-digestible cellulose. Protein, amount of protein in the diet (g/100 g total diet ingredients, both digestible and non-digestible), comprising peptone, albumin, and casein in the ratio 1:1:3. Carbs, amount of digestible carbohydrates in the diet (g/100 g total diet ingredients), in the form of sucrose. Cellulose, amount of non-digestible cellulose in the diet (g/100 g total diet ingredients). All estimates are based on the dry mass of the diet ingredients, and all other diet ingredients (linoleic acid, cholesterol, chloroform, Wesson's salts, ascorbate, and vitamin mix) are invariant across diets. Diet composition, rather than consumption, was used for logistical reasons. However, diet composition is a strong predictor of consumption in this species, in both naive and bacteria-challenged larvae (Figure S1).

the effects of host diet on the host-pathogen interaction. Most previous studies of this kind, including our own, have focused on quantifying the effects of diet on *host* survival and/or immune function [5, 8–11, 25–27]. In contrast, here we also quantify *in vivo* pathogen growth rates and age-dependent survivorship for hosts exposed to a range of doses of *X. nematophila* and fed chemically defined diets that differ in their protein:carbohydrate (P:C) ratio and/or calorie content (lipids comprise only a small proportion of the calorie intake of lepidopteran larvae and so are not varied here). Because protein and carbohydrate have similar caloric densities [30], different P:C ratios are near isocaloric, which allows the independent and interactive effects of calorie content and macronutrient composition to be statistically quantified.

We show that the outcome of this host-pathogen interaction is largely dependent on the absolute protein content of the host diet, with high-protein diets resulting in lower bacterial establishment and replication rates and slower and lower host death rates. To understand the mechanisms driving these effects, complementary *in vitro* experiments showed that high-protein diets result in host hemolymphs with high osmolalities (i.e., high concentrations of solutes), which can constrain bacterial growth rates [31]. Thus, the effects of host diet in this host-pathogen interaction appear to be mediated, to a large degree, via the direct effects of dietary protein on host hemolymph osmolality and pathogen performance, with dietary effects on the host immune system being much weaker [10]. This highlights a novel bottom-up mechanism by which diet can impact both pathogen growth and host fitness.

RESULTS

The aim of the experiments was to quantify how host macronutrient intake influences the outcome of infection through its effects on the growth of pathogen populations. Larvae were fed on one of six chemically defined diets that varied in both the P:C ratio and calorie density (Table 1). The six diets could be described with respect to the absolute amount of protein or carbohydrate or by their calorie density, ratio (P:C), interaction (P*C), or individual diet characteristics (A–F; Table 1). These diets cover the range of macronutrient levels that this generalist herbivore is likely to encounter in the wild [32, 33]. Larvae were placed on one of these six diets for 24 h before inoculation with one of four doses of *X. nematophila* (0 [control], low, medium, or high; see STAR Methods for further details). Hemolymph was sampled from a subset of larvae after infection (12, 16, 20, 24, 28, or 36 h post-challenge) for bacterial quantification and all larvae were monitored for death every hour throughout the duration of the sampling period (12–36 h) and as frequently as possible thereafter until all insects had died (as larvae, pupae, or adults). Where logistically possible, within an hour of death, hemolymph samples were also taken to ascertain bacterial load at death. We then explored in more detail the potential mechanisms involved in determining the outcome of the host-pathogen interaction.

Overall mortality in the larval stage was 84.9% (n = 270/318) in the bacterial-challenge groups and 3.6% (n = 5/141) in the non-challenged control group (none of which died due to infection by *X. nematophila*). Challenged larvae that succumbed to infection

Please cite this article in press as: Wilson et al., Osmolality as a Novel Mechanism Explaining Diet Effects on the Outcome of Infection with a Blood Parasite, Current Biology (2020), https://doi.org/10.1016/j.cub.2020.04.058

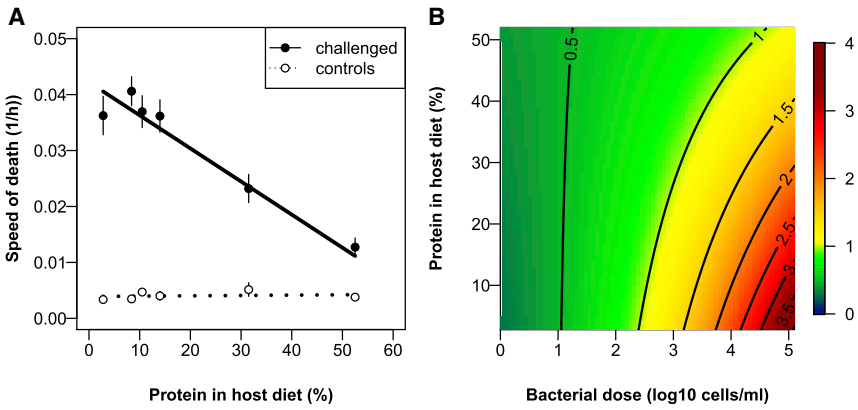

Figure 1. Relationships between the Host Dietary Protein, Bacterial Dose, and Speed of Death in Bacteria-Challenged and Non-challenged Control Insects

(A) The relationship between the amount of dietary protein and the mean (±SEM) speed of death (1/time to death in hours) averaged across bacterial doses; for a plot of speed of death versus the amount of carbohydrates in the diet, see Figure S3B (Data S1A and S1B).

(B) Heatmap showing the interactive effects of bacterial challenge dose and amount of protein in the larval diet on predicted relative mortality risk (see Data S1C–S1E and Figure S2). The interaction is reflected in the non-linear risk isoclines: at zero-low bacterial doses, relative mortality risk is low (<1) and independent of diet, whereas at higher challenge doses, mortality risk increases (>1) and diet becomes increasingly important as the amount of protein in the diet reduces (risk >>1).

did so after approximately 2 days, whereas those that either survived infection or were in the non-challenged control group lived for a further 9 days on average, usually successfully pupating and emerging as adults (mean time to death post-challenge ± SD: casualties: 42.6 ± 45.0 h, n = 270; survivors: 266.1 ± 92.2 h, n = 48; controls: 279.9 ± 100.3 h, n = 141).

Mortality Rates in Relation to Diet and Bacterial Dose

The effect of larval diet differed between challenged and control insects, with the speed of host death declining with increasing amounts of protein in the diet for bacteria-challenged larvae but being low and constant across diets for larvae in the control group (Figures 1A and S2). A survivorship model that included just the interaction between the absolute protein content of the diet (*Protein*) and the magnitude of the challenge dose (log_{10}-dose) was better (based on corrected Akaike information criteria [AIC_c] values) than all alternative models (0–9; Table 1), and it explained a similar amount of variation as the full *Diet* model (*Protein*: $r^2 = 0.434$; *Diet*: $r^2 = 0.440$; Data S1A and S1B). In contrast, the carbohydrate content of the diet explained very little variation in host speed of death (Figure S3A; Data S1A and S1B). Inspection of the predicted values for this model (and Figure 1B) revealed that the amount of protein in the diet had little effect on the hazard function of non-challenged (control) larvae: the odds ratios across diets varied between 0.289 (±0.061 SEM) and 0.388 (±0.107). In contrast, the odds of the bacteria-challenged larvae dying increased with the magnitude of the challenge dose and decreased with the amount of protein in the diet, such that when larvae were exposed to the largest bacterial challenge the odds ratio fell from 4.027 (±0.194) for larvae on the most protein-poor diet (diet A; 2.8% protein) to just 1.085 (±0.157) for those on the most protein-rich (diet F; 52.5% protein).

In Vivo Bacterial Growth Rate in Relation to Diet and Bacterial Dose

Low levels of dietary protein resulted in increased hemolymph bacterial growth rates in challenged larvae (Figure 2A), and this was especially true at the highest challenge doses where the predicted bacterial loads at 20 h differed by an order of magnitude across diets (Figure 2B). Again, the protein-dose interaction model (model 2; Table 1) had the lowest AIC_c, explaining a similar level of variation in bacterial growth rate as the full *Diet* model (*Protein*: $r^2 = 0.119$; *Diet*: $r^2 = 0.121$; Data S1C–S1E). In contrast, the hemolymph bacterial growth rate of challenged larvae was not correlated with the carbohydrate content of the host diet (model 3; Table 1; Figure S3B).

Bacterial load appeared to be determined by a two-step process. First, as indicated by the *zero-inflated* component of the model, the probability of the bacterium successfully establishing in the host (i.e., yielding a non-zero colony-forming unit [CFU] count when sampled) increased with the size of the challenge dose and decreased with the amount of protein in the diet (and the interaction between the two; Figure S4A; Data S1C–S1E). Second, as indicated by the *count* component of the model, the rate at which the bacterial population grew once established (i.e., the magnitude of the CFU count at sampling) was negatively correlated with the amount of protein in the larval diet and was independent of the size of the challenge dose (Figure S4B; Data S1C–S1E).

Bacterial Loads at Death in Relation to Diet and Bacterial Dose

At the point of death, the bacterial load of challenged larvae was a function of both the larval diet and the magnitude of the challenge dose, but the marginally best model (model 2; *Protein*) explained less than 6% of the variation in bacterial load at death ($r^2 = 0.055$; Data S1F and S1G). As expected, bacterial loads of larvae at death were significantly higher than those of the same larvae at sampling (log_{10}mean ± SD; at death, 6.01 ± 1.82; at sampling, 3.85 ± 1.74). This is consistent with larvae dying when their bacterial loads exceed some critical threshold, at around 10^6 CFU/mL (Figure 3). Of the 126 challenged larvae for which bacterial loads were quantified both as live larvae and soon after death, only nine (7%) had counts at death of less than 40,000 CFU/μL, and all but one of these had a count lower than the detection limit (the other was 1,000 CFU/mL). Bacterial loads were not quantified in the pupal or moth stages, but these results do suggest that most of the 15% of challenged larvae that successfully pupated probably did so because they were able to limit the growth of the nascent bacterial population.

Please cite this article in press as: Wilson et al., Osmolality as a Novel Mechanism Explaining Diet Effects on the Outcome of Infection with a Blood Parasite, Current Biology (2020), https://doi.org/10.1016/j.cub.2020.04.058

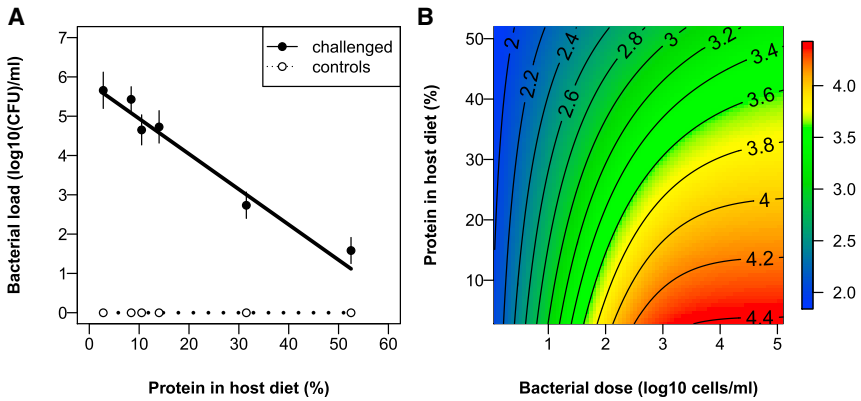

Figure 2. Relationships between the Protein Content of the Six Larval Diets, Bacterial Dose, and Bacterial Load in Bacteria-Challenged and Non-challenged Control Insects

(A) The relationship between the amount of dietary protein and the mean (±SEM) bacterial load at sampling averaged across bacterial doses. Closed symbols indicate bacteria-challenged larvae and open symbols indicate control larvae; solid and dashed lines are the fitted regression lines through the respective raw data; for a plot of bacterial load versus the amount of carbohydrates in the diet, see Figure S3B.

(B) The predicted log bacterial load at 20 h is an interactive function of the size of the challenge dose and the amount of protein in the larval diet. At zero-low bacterial doses, predicted bacterial load is low and independent of diet, whereas diet becomes increasingly important as the bacterial dose increases. See Figure S4 for the relationships between bacterial dose and the amount of protein in the diet in relation to the prevalence of bacterial infection and the bacterial load of infected larvae.

Using the restricted dataset in which bacterial counts were available both prior to and at death, the marginally best model explaining bacterial load at death was again one in which the larval diet attributes were represented by the amount of protein ($r^2 = 0.102$; Data S1H and S1I). As reflected in Figure 3, the *Protein* model revealed that the magnitude of the bacterial load at death was not significantly correlated with the rate at which the hemolymph bacterial population grew, after controlling for sampling time, diet, and challenge dose ($z = 1.415$, $p = 0.16$; Data S1H and S1I); in other words, larvae generally died if and when their bacterial load reached the critical threshold level regardless of their bacterial load at sampling.

Correlation between Mortality Rates and Bacterial Growth Rates

Bacterial growth rate (at ~20 h) was a highly significant predictor of the speed of death (Figure 4A). To explore the interaction between diet, bacterial growth rate, and mortality further, the survival analysis was repeated with bacterial load at sampling (plus time of sampling and their interaction) included as a potential explanatory variable, along with the magnitude of the challenge dose and a range of alternative dietary attributes. The best model (lowest AIC_c) was one in which diet was represented by the interaction between the calorie density and P:C ratio of the diet (model 9: $r^2 = 0.734$; Data S1J and S1K). In the second best model, diet was represented by *Protein* alone and this explained a similar level of variation in survivorship (model 2: $r^2 = 0.721$; Data S1J and S1L). In fact, each of the top five diet models explained more than 70% of the variation in survivorship (Data S1M). In each case, bacterial load at sampling was a highly significant predictor of mortality risk, but larval diet explained additional variation *over and above* that explained by its effects on *in vivo* bacterial growth rate (Data S1J and S1L). Specifically, as the (relative or absolute) amount of protein in the diet increased, so the host mortality risk declined. Thus, even after accounting for (diet-induced variation in) the *in vivo* bacterial growth rate, larvae feeding on a higher protein diet lived longer on average, with the magnitude of the effect being modulated by the size of the challenge dose (Figure 4B).

Correlation between Bacterial Growth Rates and Hemolymph Osmolality

The previous experiments suggest that increased dietary protein leads to the inhibition of the growth of bacteria within the host hemolymph. Previous studies using this system suggest that some (but not all) aspects of the host immune system are upregulated on high-protein diets, but the effects are relatively weak, with diet explaining less than 10% of the variation in immune function [10]. To examine potential bottom-up effects of protein availability on bacterial growth rates in the absence of a host immune response, we created synthetic hemolymphs that mimicked the blood of hosts feeding on a range of diets that varied in their protein and carbohydrate content [34] and measured bacterial growth rates (as measured by maximum absorbance using a spectrophotometer). As predicted, bacterial growth rates declined with dietary protein content (linear model [LM]: $F_{1,57} = 16.13$, $p < 0.001$; Figure 5A; Data S1N) but carbohydrate content had no effect (LM: carbohydrate: $F_{1,56} = 0.93$, $p = 0.337$; C*P: $F_{1,55} = 1.72$, $p = 0.195$; Figure S3C; Data S1N).

In free-living bacteria, it is well established that bacterial growth rate is affected by the osmolality of the environment, with some bacterial species/strains being better than others at coping with osmotic stress [35]. To establish whether this could provide a mechanism to explain the observed patterns, we first quantified the *in vivo* hemolymph osmolality of larvae fed on each of our six diets. We observed that as the amount of dietary protein increased, there was a strong non-linear increase in the osmolality of the host hemolymph (LM: $F_{2,57} = 44.26$, $p < 0.0001$; Figure 5B; Data S1O). In contrast, there was no correlation between the amount of dietary carbohydrate and hemolymph osmolality (LM: $F_{1,58} = 0.0845$, $p = 0.77$; Figure S3D).

To establish whether this increase in hemolymph osmolality could explain why bacterial growth rates declined with increasing dietary protein, we next quantified *in vitro* bacterial growth rate across a range of synthetic hemolymphs based on Grace's insect medium, in which osmolality was altered by changing the amount of potassium chloride (KCl) in the solution. Using these synthetic hemolymphs allowed us to assess the effects of osmolality on bacterial growth in the absence of other host factors, such as immune responses. This revealed that

Please cite this article in press as: Wilson et al., Osmolality as a Novel Mechanism Explaining Diet Effects on the Outcome of Infection with a Blood Parasite, Current Biology (2020), https://doi.org/10.1016/j.cub.2020.04.058

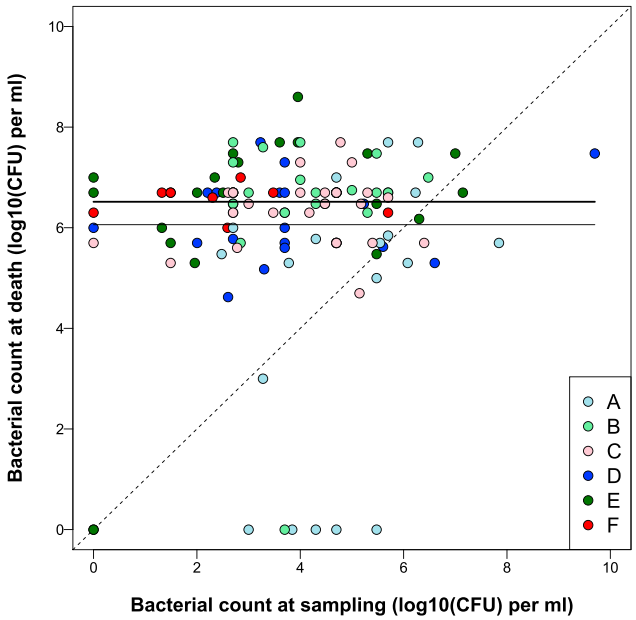

Figure 3. Relationship between Bacterial Load at Sampling and Bacterial Load at Death

Different-colored symbols refer to the six different diets (A–F; Table 1). The dashed diagonal line is the line of parity (1:1) for bacterial counts at sampling and at death. The thin horizontal line is the mean bacterial count at death, across all diets, when the nine very low counts ($<10^1$) are included; the thick line is the mean when these are excluded (Data S1F–S1I).

X. nematophila growth rate (as measured by maximum absorbance using a spectrophotometer) was a non-linear function of the osmolality of the growth medium, peaking at around 200 mOsmol/kg (generalized additive model [GAM]: F = 168.9, edf = 7.846, Ref.df = 8.53, $p < 0.0001$, $r^2 = 0.978$; Figure 5C; Data S1P). Moreover, over the range of osmolalities observed for *S. littoralis* hemolymph in the previous experiment (240–350 mOsmol/kg; black symbols in Figure 5C), *X. nematophila* growth rate declined linearly with increasing osmolality (LM: $F_{1,13} = 21.302$, $p = 0.00048$). This strongly suggests that the declining bacterial growth rates and host mortality rates observed with increasing dietary protein are explained, in part at least, by the effect of dietary protein on host hemolymph osmolality.

To test this more directly, we produced three new host diets based on the low-protein diet A from the previous experiments. These new diets (A3, A6, and A8) had Wesson's salts added to increase their predicted hemolymph osmolalities from 251 mOsmol/kg to 282, 302, and 325 mOsmol/kg, respectively. Larvae were fed one of each of these four diets or diets C, E, or F, and then *X. nematophila* growth was quantified at ~20 h post-challenge. As predicted, bacterial load at sampling was negatively related to the osmolality of the hemolymph (LM: $F_{1,29} = 8.44$, $p = 0.007$), regardless of whether osmolality was manipulated by the addition of dietary proteins or salts (Figure 5D; Data S1Q).

DISCUSSION

Here, through experimental manipulation of both the calorie content and macronutrient composition of the larval diet, we have shown the central role that protein plays in determining the outcome of an insect host-pathogen interaction. In contrast to previous studies in this field (e.g., [5, 9–11, 25]), most of which have focused on host mortality and immune function under different dietary regimes, here we explored the effects of diet from the perspectives of both the host and the pathogen. This revealed that the *in vivo* replication rate of the bacteria declined as a linear function of the absolute amount of protein in the larval diet, and that this was correlated with a parallel reduction in the bacteria-induced larval mortality rate. Moreover, we identify a novel bottom-up mechanism by which host diet influences pathogen and host fitness via changes in the level of osmotic stress experienced by replicating bacteria within the host's hemolymph.

For all the metrics studied here (host survivorship, bacterial establishment, bacterial replication rate, and, to a lesser extent, bacterial load at death), protein consistently emerged as the pre-eminent nutritional attribute determining the outcome of the host-pathogen interaction. In contrast, dietary carbohydrate appeared to have a negligible effect on host or pathogen fitness, usually explaining a minimal amount of variation. Protein also consistently out-performed the calorie content of the diet, indicating that it is the specific nutritional source of those calories that is the prime determinant of host and pathogen performance.

The present study is one of the few to quantify *in vivo* pathogen performance in relation to host diet (but see [22, 36–40]). It clearly demonstrates that the bacterial replication rate declines as a linear function of the amount of protein in the larval diet, with larvae on the lowest-protein diet harboring bacterial loads that were on average 3.6 orders of magnitude higher than those of larvae on the highest-protein diet. If the relationship between dietary protein and bacterial load is log linear across all protein concentrations (Figure 2A), it is predicted that larvae would be virtually bacteria free, on average, if they were fed diets exceeding 69 g protein per 100 g diet.

The slower growth rate of bacteria on high-protein diets could be because they are being suppressed by a host immune system that mostly relies on protein-dependent immune effectors (i.e., top-down regulation [12]). Previous work on *Spodoptera* spp. suggests that whereas some immune effector systems are weakly upregulated on protein-rich diets, others appear to be either carbohydrate dependent or relatively independent of diet [5, 6, 10, 25, 26, 41]. In this system at least, it therefore seems unlikely that immune regulation of bacterial growth is a key factor determining the outcome of the host-pathogen interaction. However, a possible bottom-up effect that could regulate bacterial proliferation *in vivo* is that host diet affects the (non-immune) environmental stresses experienced by the pathogen. Specifically, here we show that the increased presence of solutes in the hemolymph of larvae feeding on protein-rich diets dramatically increases its osmolality, an effect that has also been observed in migratory locusts, *Locusta migratoria*, which the authors attributed to higher levels of free amino acids in the blood [42].

It is well established that free-living bacteria can be prone to osmotic stress, as increased osmolality tends to withdraw water from cells, decreasing their turgor pressure and raising concentrations of intracellular solutes to levels that can inhibit growth

Please cite this article in press as: Wilson et al., Osmolality as a Novel Mechanism Explaining Diet Effects on the Outcome of Infection with a Blood Parasite, Current Biology (2020), https://doi.org/10.1016/j.cub.2020.04.058

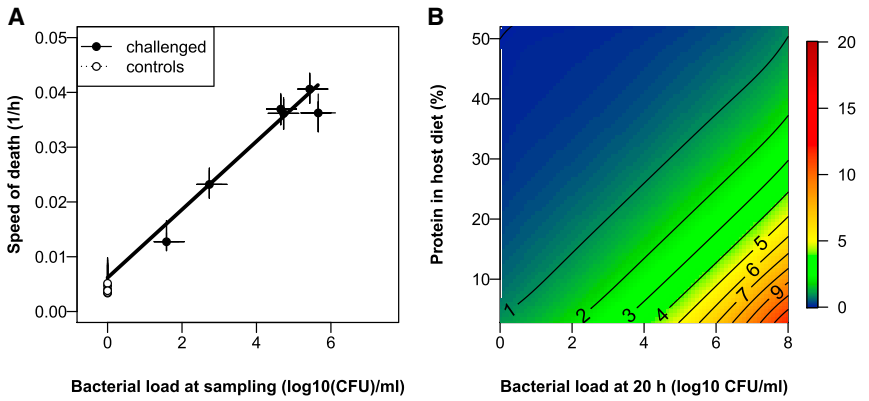

Figure 4. Relationships between Dietary Protein Content, Bacterial Load, and Larval Mortality

(A) The relationship between bacterial load at sampling (means ± SEM) and speed of death (means ± SEM) across the six diets for control (open symbols) and bacteria-challenged insects (closed symbols). The solid line is the fitted regression line through the raw data.

(B) Heatmap showing the interactive effects of bacterial load (standardized to mean load at 20 h post-challenge) and the amount of protein in the larval diet on predicted relative mortality risk. Figures are based on predictions from the model described in Data S1L. For illustrative purposes, predictions are shown for a high challenge dose (≥1,000 bacterial cells/mL); for lower challenge doses, the figure is qualitatively the same but the magnitudes of the risks are reduced (and heatmap colors are cooler). Mortality risk increases with the magnitude of the bacterial load at 20 h and decreases as the amount of dietary protein increases.

[35]. However, as far as we are aware, the effects of hemolymph osmolality on the regulation of blood parasites have not previously been explored. Here we show that over the range of osmolalities observed in *S. littoralis* hemolymph, *in vitro* growth of *X. nematophila* was negatively related to environmental osmolality and that when hemolymph osmolality was manipulated by changing dietary levels of salts or proteins, this was reflected in the *in vitro* bacterial growth rates. These results suggest that the negative effects of dietary protein on bacterial proliferation are largely independent of any top-down host immune responses [10] and are instead most likely mediated via their effects on hemolymph osmolality. Of course, sugars are also solutes that could alter hemolymph osmolality, but these are much more tightly regulated by insects than are amino acids and proteins [43] and our results suggest that dietary carbohydrates do not significantly influence bacterial growth rates (Figure S3). We cannot, at this stage, exclude the possibility that something other than osmolality is driving the observed patterns (e.g., levels of hemolymph uric acid, xanthine oxidase activity, etc.) but we feel that, given the well-established susceptibility of free-living bacteria to osmotic stress, this is the most parsimonious interpretation of our current findings. Future studies will explore these other possibilities.

Bacterial loads at death were relatively invariant and largely independent of diet (Figure 3), with the amount of protein in the larval diet explaining less than 6% of the variation in mortality. Thus, it appears that dietary protein determines the *rate* at which bacteria replicate within host hemolymph, as well as their establishment success, and that the insect dies if and when the bacterial density exceeds a critical threshold (at around 10^6 CFU/mL hemolymph). This is possibly because the concentration of bacteria-produced toxins causes lethal host tissue degradation and/or because there are simply too few resources remaining for the operation of essential host processes [29]. Across all bacterial doses, there was a strong log-linear relationship between bacterial load at <20 h and the average speed at which insects died (Figure 4A). On average there was a 3-fold difference in the rate at which bacteria-challenged insects died across the different dietary treatments, with those on the highest-protein diet living for an average of 78 h compared to just 27 h for those on the lowest-protein diet (Figure 1A).

How general is our finding that dietary protein impacts host-pathogen interactions? Our results are consistent with previous work on *Spodoptera* spp. using other pathogens [5, 25, 26], all of which has documented that host survival is enhanced on protein-biased isocaloric diets. They are also consistent with the limited number of previous studies that have addressed this question in vertebrate host-pathogen systems. For example, Peck et al. [20] observed that mortality in lab mice infected with *Salmonella typhimurium* decreased from 100% on protein-poor (carbohydrate-rich) diets to just 40% on protein-rich (carbohydrate-poor) diets. Our findings are also not at odds with studies that have observed a positive effect of calorie intake on parasite resistance [44–47], because high-calorie diets will also contain high levels of protein. Indeed, much of the human literature has focused on the exacerbating effects of "protein-energy malnutrition" on infectious diseases, especially in children [48–50]. Thus, it is possible that the positive effects of protein on survival following infection is a widespread (although not ubiquitous [9, 11, 18, 19, 23, 24]) phenomenon, but it is only by making comparisons in different host-pathogen systems across a range of diets that span sufficiently large regions of the organism's nutritional landscape that such generalities will emerge.

In summary, this study provides new insights into the effects of host diet on the dynamics of the host-pathogen interaction from the perspective of both the pathogen and its host. We have shown how *in vivo* pathogen growth rate varies with host diet and predicts host survivorship. We are beginning to get an appreciation of the range of diet-driven mechanisms that combine to determine the outcome of host-pathogen interactions, and the current study provides a novel (stress-related) mechanism to add into the mix. Human blood also exhibits natural variation in osmolality (usual range: 275–295 mOsmol/kg [51]; in dehydrated individuals: >300 mOsmol/kg [52]) but it remains to be established whether this impacts the dynamics of human-blood parasite interactions. There is clear scope for determining whether the blood parasites of humans (e.g., *Plasmodium* causing malaria and bacteria causing septicemia) could

Please cite this article in press as: Wilson et al., Osmolality as a Novel Mechanism Explaining Diet Effects on the Outcome of Infection with a Blood Parasite, Current Biology (2020), https://doi.org/10.1016/j.cub.2020.04.058

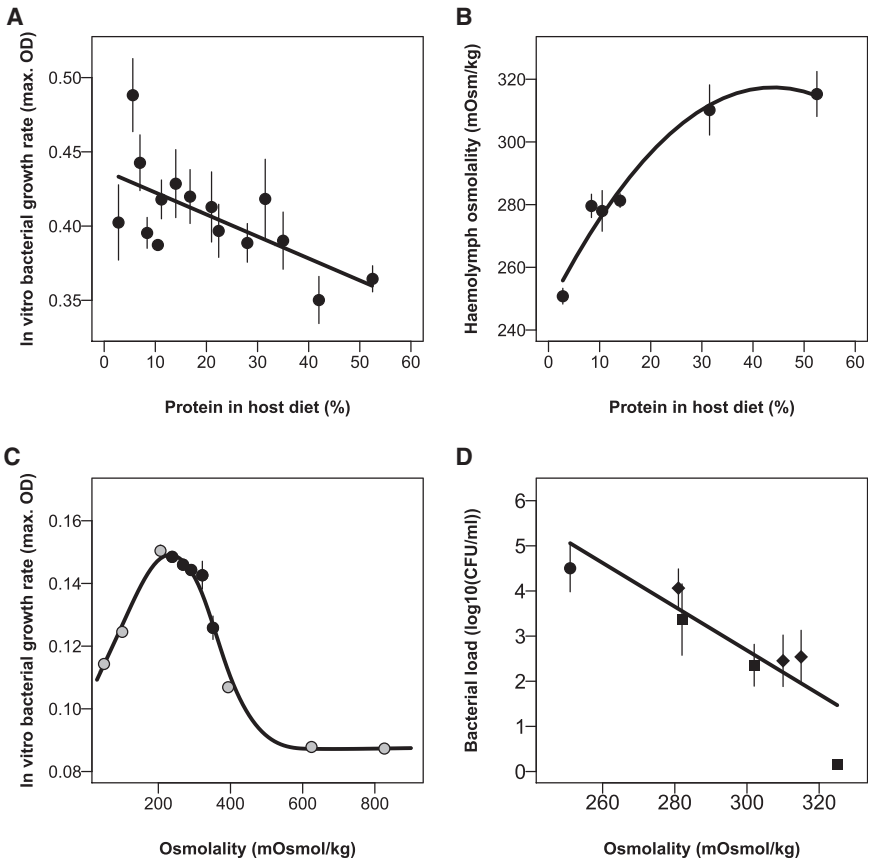

Figure 5. The Relationship between Protein, Osmolality, and Bacterial Growth Rates

(A) Bacterial growth rate *in vitro* decreases with the protein content of the host diet; for the equivalent plot in relation to the amount of carbohydrates in the diet, see Figure S3C. The points represent the mean (±SEM) for larvae fed on one of 20 chemically defined diets, and the solid line is the fitted quadratic regression line through the raw data.

(B) Dietary protein increases the *in vivo* osmolality of host hemolymph; for the equivalent plot in relation to the amount of carbohydrates in the diet, see Figure S3D. The points represent the mean (±SEM) for larvae fed on the 6 diets and the solid line is the fitted quadratic regression line through the raw data.

(C) Bacterial growth rate *in vitro* initially increased with the osmolality of the growth media before falling sharply. The line represents the fitted curve obtained from the GAM. All symbols represent the mean (±SEM) of replicate bacterial populations; black symbols represent those for which the osmolality is within the range observed for *S. littoralis* hemolymph.

(D) Bacterial growth rate *in vivo* decreased with the osmolality of the hemolymph, irrespective of whether this was achieved via the addition to diet A (circle, 2.8% protein) of protein (diamonds, left to right: 14.0%, 31.5%, 52.5% protein) or salt (squares, left to right: 7.5%, 15%, 20% Wesson's salts). The points represent the mean (±SEM); the line is the fitted linear regression through the raw data.

For details of the models, see Data S1N–S1Q.

be managed via the manipulation of blood osmolality, but it is pertinent to note that one of the immediate treatments for sepsis is the intravenous administration of a saline solution or some other crystalloid/colloid fluid, primarily to increase blood volume [53, 54].

STAR★METHODS

Detailed methods are provided in the online version of this paper and include the following:

- KEY RESOURCES TABLE
- RESOURCE AVAILABILITY
  - Lead Contact
  - Materials Availability
  - Data and Code Availability
- EXPERIMENTAL MODEL AND SUBJECT DETAILS
  - Host: Spodoptera littoralis
  - Pathogen: Xenorhabdus nematophila F1D3
- METHOD DETAILS
  - Main experimental design
- QUANTIFICATION AND STATISTICAL ANALYSIS
  - Survivorship
  - *In vivo* bacterial growth rate
  - Bacterial loads at death
  - Correlation between survivorship and bacterial growth rates
  - Correlation between bacterial growth rates and hemolymph osmolality

SUPPLEMENTAL INFORMATION

Supplemental Information can be found online at https://doi.org/10.1016/j.cub.2020.04.058.

ACKNOWLEDGMENTS

This study was funded by a research grant awarded to K.W., J.A.S., and S.J.S. by the United Kingdom's Biotechnology and Biological Sciences Research Council (BB/I02249X/1). S.C.C. was supported by a Natural Environment Research Council independent research fellowship (NE/H014225/2). We are grateful to Alain Givaudan and colleagues (Montpellier University, France) for supplying and advising on the GFP-labeled *X. nematophila* F1D3 bacteria, and to Esmat Hegazi for support with *S. littoralis* stocks. We thank Phill Nott for technical assistance.

AUTHOR CONTRIBUTIONS

K.W., J.A.S., S.J.S., and S.C.C. conceived the research idea. The experiments were designed by K.W., R.H., S.C.C., C.E.R., and J.L.R. and were carried out by R.H., C.E.R., and Y.T. The data were analyzed by R.H., K.W., and S.C.C. Early drafts of the manuscript were written by R.H., K.W., C.E.R., and S.C.C.; all authors contributed to the final draft.

DECLARATION OF INTERESTS

The authors declare no competing interests.

Received: January 27, 2020
Revised: March 19, 2020
Accepted: April 22, 2020
Published: June 4, 2020

REFERENCES

1. Calder, P.C., and Jackson, A.A. (2000). Undernutrition, infection and immune function. Nutr. Res. Rev. *13*, 3–29.
2. Cunningham-Rundles, S., McNeeley, D.F., and Moon, A. (2005). Mechanisms of nutrient modulation of the immune response. J. Allergy Clin. Immunol. *115*, 1119–1128, quiz 1129.
3. Ponton, F., Wilson, K., Cotter, S.C., Raubenheimer, D., and Simpson, S.J. (2011). Nutritional immunology: a multi-dimensional approach. PLoS Pathog. *7*, e1002223.
4. Ponton, F., Wilson, K., Holmes, A.J., Cotter, S.C., Raubenheimer, D., and Simpson, S.J. (2013). Integrating nutrition and immunology: a new frontier. J. Insect Physiol. *59*, 130–137.
5. Povey, S., Cotter, S.C., Simpson, S.J., Lee, K.P., and Wilson, K. (2009). Can the protein costs of bacterial resistance be offset by altered feeding behaviour? J. Anim. Ecol. *78*, 437–446.
6. Cotter, S., Simpson, S., Raubenheimer, D., and Wilson, K. (2011). Macronutrient balance mediates trade-offs between immune function and life history traits. Funct. Ecol. *25*, 186–198.
7. Brunner, F.S., Schmid-Hempel, P., and Barribeau, S.M. (2014). Protein-poor diet reduces host-specific immune gene expression in *Bombus terrestris*. Proc. Biol. Sci. *281*, 20140128.
8. Kay, A.D., Bruning, A.J., van Alst, A., Abrahamson, T.T., Hughes, W.O.H., and Kaspari, M. (2014). A carbohydrate-rich diet increases social immunity in ants. Proc. Biol. Sci. 281, 20132374.
9. Galenza, A., Hutchinson, J., Campbell, S.D., Hazes, B., and Foley, E. (2016). Glucose modulates *Drosophila* longevity and immunity independent of the microbiota. Biol. Open *5*, 165–173.
10. Cotter, S.C., Reavey, C.E., Tummala, Y., Randall, J.L., Holdbrook, R., Ponton, F., Simpson, S.J., Smith, J.A., and Wilson, K. (2019). Diet modulates the relationship between immune gene expression and functional immune responses. Insect Biochem. Mol. Biol. *109*, 128–141.
11. Ponton, F., Morimoto, J., Robinson, K., Kumar, S.S., Cotter, S.C., Wilson, K., and Simpson, S.J. (2020). Macronutrients modulate survival to infection and immunity in *Drosophila*. J. Anim. Ecol. *89*, 460–470.
12. Haydon, D.T., Matthews, L., Timms, R., and Colegrave, N. (2003). Top-down or bottom-up regulation of intra-host blood-stage malaria: do malaria parasites most resemble the dynamics of prey or predator? Proc. Biol. Sci. *270*, 289–298.
13. Mideo, N., Barclay, V.C., Chan, B.H., Savill, N.J., Read, A.F., and Day, T. (2008). Understanding and predicting strain-specific patterns of pathogenesis in the rodent malaria *Plasmodium chabaudi*. Am. Nat. *172*, 214–238.
14. Metcalf, C.J.E., Graham, A.L., Huijben, S., Barclay, V.C., Long, G.H., Grenfell, B.T., Read, A.F., and Bjørnstad, O.N. (2011). Partitioning regulatory mechanisms of within-host malaria dynamics using the effective propagation number. Science *333*, 984–988.
15. Griffiths, E.C., Fairlie-Clarke, K., Allen, J.E., Metcalf, C.J.E., and Graham, A.L. (2015). Bottom-up regulation of malaria population dynamics in mice co-infected with lung-migratory nematodes. Ecol. Lett. *18*, 1387–1396.
16. Ramiro, R.S., Pollitt, L.C., Mideo, N., and Reece, S.E. (2016). Facilitation through altered resource availability in a mixed-species rodent malaria infection. Ecol. Lett. *19*, 1041–1050.
17. Freitak, D., Ots, I., Vanatoa, A., and Horak, P. (2003). Immune response is energetically costly in white cabbage butterfly pupae. Proc. Biol. Sci. *270*, S220–S222.
18. Srygley, R.B., and Lorch, P.D. (2011). Weakness in the band: nutrient-mediated trade-offs between migration and immunity of Mormon crickets, *Anabrus simplex*. Anim. Behav. *81*, 395–400.
19. Graham, R.I., Deacutis, J.M., Pulpitel, T., Ponton, F., Simpson, S.J., and Wilson, K. (2014). Locusts increase carbohydrate consumption to protect against a fungal biopesticide. J. Insect Physiol. *69*, 27–34.
20. Peck, M.D., Babcock, G.F., and Alexander, J.W. (1992). The role of protein and calorie restriction in outcome from *Salmonella* infection in mice. JPEN J. Parenter. Enteral Nutr. *16*, 561–565.
21. Nnadi, P.A., Ezeh, I.O., Kalu, K.C., and Ngene, A.A. (2010). The impact of dietary protein on the pathophysiology of porcine trypanosome infection. Vet. Parasitol. *173*, 193–199.
22. Sakkas, P., Houdijk, J.G.M., Jones, L.A., Knox, D.P., and Kyriazakis, I. (2011). Dietary protein and energy supplies differentially affect resistance to parasites in lactating mammals. Br. J. Nutr. *106*, 1207–1215.
23. Cheon, H.-M., Shin, S.W., Bian, G., Park, J.-H., and Raikhel, A.S. (2006). Regulation of lipid metabolism genes, lipid carrier protein lipophorin, and its receptor during immune challenge in the mosquito *Aedes aegypti*. J. Biol. Chem. *281*, 8426–8435.
24. Adamo, S.A., Roberts, J.L., Easy, R.H., and Ross, N.W. (2008). Competition between immune function and lipid transport for the protein apolipophorin III leads to stress-induced immunosuppression in crickets. J. Exp. Biol. *211*, 531–538.
25. Lee, K.P., Cory, J.S., Wilson, K., Raubenheimer, D., and Simpson, S.J. (2006). Flexible diet choice offsets protein costs of pathogen resistance in a caterpillar. Proc. Biol. Sci. *273*, 823–829.
26. Povey, S., Cotter, S.C., Simpson, S.J., and Wilson, K. (2014). Dynamics of macronutrient self-medication and illness-induced anorexia in virally infected insects. J. Anim. Ecol. *83*, 245–255.
27. Dinh, H., Mendez, V., Tabrizi, S.T., and Ponton, F. (2019). Macronutrients and infection in fruit flies. Insect Biochem. Mol. Biol. *110*, 98–104.
28. Georgis, R., Koppenhöfer, A., Lacey, L., Bélair, G., Duncan, L., Grewal, P., Samish, M., Tan, L., Torr, P., and Van Tol, R. (2006). Successes and failures in the use of parasitic nematodes for pest control. Biol. Control *38*, 103–123.
29. Herbert, E.E., and Goodrich-Blair, H. (2007). Friend and foe: the two faces of *Xenorhabdus nematophila*. Nat. Rev. Microbiol. *5*, 634–646.
30. Merrill, A.L., and Watt, B.K. (1973). Energy Value of Foods: Basis and Derivation. Agriculture Handbook no. 74 (U.S. Department of Agriculture).
31. Record, M.T., Jr., Courtenay, E.S., Cayley, D.S., and Guttman, H.J. (1998). Responses of *E. coli* to osmotic stress: large changes in amounts of cytoplasmic solutes and water. Trends Biochem. Sci. *23*, 143–148.
32. Brown, A.S., Simmonds, M.S.J., and Blaney, W.M. (2002). Relationship between nutritional composition of plant species and infestation levels of thrips. J. Chem. Ecol. *28*, 2399–2409.
33. Wilson, J.K., Ruiz, L., Duarte, J., and Davidowitz, G. (2019). The nutritional landscape of host plants for a specialist insect herbivore. Ecol. Evol. *9*, 13104–13113.
34. Holdbrook, R. (2019). Nutrition modulates the interaction between the bacterium Xenorhabdus nematophila and its lepidopteran host Spodoptera littoralis. PhD thesis (Lancaster University).
35. Singleton, P. (2004). Bacteria in Biology, Biotechnology and Medicine, Fifth Edition (Wiley).
36. Kambara, T., McFarlane, R.G., Abell, T.J., McAnulty, R.W., and Sykes, A.R. (1993). The effect of age and dietary protein on immunity and resistance in lambs vaccinated with *Trichostrongylus colubriformis*. Int. J. Parasitol. *23*, 471–476.
37. Frost, P.C., Ebert, D., and Smith, V.H. (2008). Responses of a bacterial pathogen to phosphorus limitation of its aquatic invertebrate host. Ecology *89*, 313–318.
38. Narr, C.F., and Krist, A.C. (2015). Host diet alters trematode replication and elemental composition. Freshw. Sci. *34*, 81–91.
39. Kutzer, M.A.M., and Armitage, S.A.O. (2016). The effect of diet and time after bacterial infection on fecundity, resistance, and tolerance in *Drosophila melanogaster*. Ecol. Evol. *6*, 4229–4242.

40. Miller, C.V.L., and Cotter, S.C. (2018). Resistance and tolerance: the role of nutrients on pathogen dynamics and infection outcomes in an insect host. J. Anim. Ecol. *87*, 500–510.

41. Lee, K.P., Simpson, S.J., and Wilson, K. (2008). Dietary protein-quality influences melanization and immune function in an insect. Funct. Ecol. *22*, 1052–1061.

42. Abisgold, J.D., and Simpson, S.J. (1987). The physiology of compensation by locusts for changes in dietary protein. J. Exp. Biol. *129*, 329–346.

43. Chapman, R., Simpson, S., and Douglas, A. (2013). The Insects: Structure and Function, Fifth Edition (Cambridge University Press).

44. Moret, Y., and Schmid-Hempel, P. (2000). Survival for immunity: the price of immune system activation for bumblebee workers. Science *290*, 1166–1168.

45. Anstead, G.M., Chandrasekar, B., Zhao, W., Yang, J., Perez, L.E., and Melby, P.C. (2001). Malnutrition alters the innate immune response and increases early visceralization following *Leishmania donovani* infection. Infect. Immun. *69*, 4709–4718.

46. Kristan, D.M. (2007). Chronic calorie restriction increases susceptibility of laboratory mice (*Mus musculus*) to a primary intestinal parasite infection. Aging Cell *6*, 817–825.

47. Kristan, D.M. (2008). Calorie restriction and susceptibility to intact pathogens. Age (Dordr.) *30*, 147–156.

48. Blössner, M., and de Onis, M. (2005). WHO Environmental Burden of Disease Series, no. 12 (World Health Organization).

49. Gordon, B.A., Mackay, R., and Rehfuess, E. (2004). Inheriting the World: The Atlas of Children's Health and the Environment (World Health Organization).

50. Bryce, J., Boschi-Pinto, C., Shibuya, K., and Black, R.E.; WHO Child Health Epidemiology Reference Group (2005). WHO estimates of the causes of death in children. Lancet *365*, 1147–1152.

51. Kaya, H., Yücel, O., Ege, M.R., Zorlu, A., Yücel, H., Güneş, H., Ekmekçi, A., and Yılmaz, M.B. (2017). Plasma osmolality predicts mortality in patients with heart failure with reduced ejection fraction. Kardiol. Pol. *75*, 316–322.

52. Hooper, L., Abdelhamid, A., Ali, A., Bunn, D.K., Jennings, A., John, W.G., Kerry, S., Lindner, G., Pfortmueller, C.A., Sjöstrand, F., et al. (2015). Diagnostic accuracy of calculated serum osmolarity to predict dehydration in older people: adding value to pathology laboratory reports. BMJ Open *5*, e008846.

53. Avila, A.A., Kinberg, E.C., Sherwin, N.K., and Taylor, R.D. (2016). The use of fluids in sepsis. Cureus *8*, e528.

54. Rhodes, A., Evans, L.E., Alhazzani, W., Levy, M.M., Antonelli, M., Ferrer, R., Kumar, A., Sevransky, J.E., Sprung, C.L., Nunnally, M.E., et al. (2017). Surviving Sepsis Campaign: International Guidelines for Management of Sepsis and Septic Shock: 2016. Intensive Care Med. *43*, 304–377.

55. R Core Team (2018). R: a language and environment for statistical computing (R Foundation for Statistical Computing).

56. Whittingham, M.J., Stephens, P.A., Bradbury, R.B., and Freckleton, R.P. (2006). Why do we still use stepwise modelling in ecology and behaviour? J. Anim. Ecol. *75*, 1182–1189.

57. Bartoń, K. (2018). MuMIn: multi-model inference. R package version 1.42.1 (CRAN.R-project.org). https://cran.r-project.org/.

58. Therneau, T. (2015). A package for survival analysis in S R package version 3.1-12 (CRAN.R-project.org). https://CRAN.R-project.org/package=survival.

59. Nychka, D., Furrer, R., Paige, J., and Sain, S. (2017). Fields: tools for spatial data. R package version 9.6 R package version 10.3 (CRAN.R-project.org). https://github.com/NCAR/Fields.

60. Zeileis, A., Kleiber, C., and Jackman, S. (2008). Regression models for count data in R. J. Stat. Softw. *27*, 1–25.

61. Jackman, S. (2017). pscl: classes and methods for R developed in the political science computational laboratory. R package version 1 (United States Studies Centre, University of Sydney).

62. Venables, W., and Ripley, B. (2002). Modern Applied Statistics with S (Springer).

63. Wood, S.N. (2011). Fast stable restricted maximum likelihood and marginal likelihood estimation of semiparametric generalized linear models. J. R. Stat. Soc. Series B Stat. Methodol. *73*, 3–36.

Please cite this article in press as: Wilson et al., Osmolality as a Novel Mechanism Explaining Diet Effects on the Outcome of Infection with a Blood Parasite, Current Biology (2020), https://doi.org/10.1016/j.cub.2020.04.058

STAR★METHODS

KEY RESOURCES TABLE

REAGENT or RESOURCE	SOURCE	IDENTIFIER
Bacterial and Virus Strains		
GFP-labeled *Xenorhabdus nematophila* F1D3	Alain Givaudan and colleagues (Montpellier University, France)	N/A
Deposited Data		
All raw data generated	Mendeley Data	v1 https://doi.org/10.17632/g74dpzb7g8.1
Experimental Models: Organisms/Strains		
Spodoptera littoralis (Lepidoptera: Noctuidae) - Egypt	This study	N/A
Software and Algorithms		
R ver. 3.5.1	CRAN	https://www.r-project.org/
SURVIVAL	CRAN	https://cran.r-project.org/web/packages/survival/
FIELDS	CRAN	https://cran.r-project.org/web/packages/fields/
MUMIN	CRAN	https://cran.r-project.org/web/packages/MuMin/
MGCV	CRAN	https://cran.r-project.org/web/packages/mgcv/
GAM	CRAN	https://cran.r-project.org/web/packages/gam/
PSCL	CRAN	https://cran.r-project.org/web/packages/pscl
MASS	CRAN	https://cran.r-project.org/web/packages/mass/
Magellan v7.2	Tecan	https://lifesciences.tecan.com/software-magellan
Other		
Microscope, Compound, Zeiss Axioskop 40 Fluorescent	Carl Zeiss Ltd	Cat# Axopskop40FL-1
Microtiter Plate Reader, Tecan Infinite 200 Pro	Tecan /Labtech	Cat#INF-FPLEX
Microinjector, Pump 11 Elite Nanomite Programmable Syringe Pump	Harvard Apparatus	Cat#70-4507
Hamilton syringe needle (gauge = 0.5 mm)	Sigma-Aldrich	Cat# 20734
Osmometer, Osmomat 3000 basic	Gonotec / Wolflabs	Cat#32.B

RESOURCE AVAILABILITY

Lead Contact

Further information and requests for resources and reagents should be directed to and will be fulfilled by the Lead Contact, Kenneth Wilson (ken.wilson@lancaster.ac.uk).

Materials Availability

This study did not generate new unique reagents.

Data and Code Availability

All raw data have been deposited in Mendeley Data: https://doi.org/10.17632/g74dpzb7g8.1.

EXPERIMENTAL MODEL AND SUBJECT DETAILS

Host: Spodoptera littoralis

The *S. littoralis* culture was established from eggs collected near Alexandria in Egypt in 2011 and has since been maintained using single pair matings of non-relatives for *c*. 40 generations, with around 150 pairs each generation to reduce inbreeding. Larvae were reared individually from the 2nd larval instar on a semi-artificial wheatgerm-based diet in 25 mL polypots. *S. littoralis* spend approximately two weeks in the larval stage, about seven days of which are spent in the 5th and 6th instars. Insects were maintained at 25°C under a 12:12 light: dark photo regime. It is not possible to establish the sex of the larvae used.

Please cite this article in press as: Wilson et al., Osmolality as a Novel Mechanism Explaining Diet Effects on the Outcome of Infection with a Blood Parasite, Current Biology (2020), https://doi.org/10.1016/j.cub.2020.04.058

Pathogen: Xenorhabdus nematophila F1D3

Pure X. nematophila F1D3 stocks gifted by Alain Givaudan were stored at −20°C in 1.5 mL microtubes (500 μl of X. nematophila in nutrient broth with 500 μl of glycerol). Vortexing ensured that all X. nematophila cells were coated in glycerol. To revive the stocks for use, 100 μl was added to 10 mL nutrient broth, and incubated at 28°C for up to 48 h (generally stocks had grown sufficiently after 24 h). On the day of experimental bacterial challenge, the stock was sub-cultured, with 1 mL of the original stock added to 10 mL of nutrient broth and placed in a shaker-incubator for approximately 4 h. This ensured that the bacteria were in log phase prior to challenge. Following the sub-culture, a 1 mL sample was first checked for purity and then used to produce a serial dilution in nutrient broth, from which the total cell count was determined with fluorescence microscopy, using a hemocytometer with improved Neubauer ruling. The remaining culture was diluted with nutrient broth to the appropriate concentration required for the bacterial challenge.

METHOD DETAILS

Main experimental design

A total of 468 larvae were first reared to the start of final larval instar on a semi-artificial wheat germ-based diet [25]. Within 24 h of moulting, the larvae were divided into six groups (n = 78 per group) and placed onto one of the six chemically defined diets (A–F; Table 1). Approximately 1.5 g of the chemically defined diets was placed in 90 mm diameter Petri dishes. Within each diet, 24 larvae were allocated to the control group (no bacterial challenge) and 54 were assigned to the bacteria-challenged group. Following 24 h feeding on the assigned diets (at time, t = 0 h), each of the 324 bacteria-challenged larvae was injected with 5 μl of one of three bacterial solutions (averaging 1975, 5089 and 123300 *X. nematophila* cells per mL nutrient broth) using a microinjector (Pump 11 Elite Nanomite) fitted with a Hamilton syringe (gauge = 0.5mm). The syringe was sterilized in ethanol prior to use and the challenge was applied to the left anterior proleg. Injecting the 324 challenged larvae took approximately 3 h and time of injection was recorded but did not influence any of the metrics reported here. Survivorship does not differ between larvae injected with heat-killed bacteria and larvae that are handled but not injected (Figure S5), and so for logistical reasons the control larvae were handled at this time but not injected.

Within each diet treatment group, nine of the challenged larvae were assigned to each of the following times for hemolymph sampling: 12, 16, 20, 24, 28 or 36 h post-challenge (t = 0 h); in the control group, twelve larvae from each diet were sampled after either 20 h or 36 h (none of these died of *X. nematophila* infection). Hemolymph samples were obtained by piercing the cuticle next to the left anterior proleg with a sterile needle and allowing released hemolymph to bleed directly into a microtube. Immediately following sampling, each sample was diluted 1:9 in pH 7.4 phosphate buffered saline, PBS, and a dilution series produced down to 10^{-7} in intervals of 10^{-1}. The dilution series was plated onto NBTL agar plates (20 μl per 1/4 agar plate), incubated at 28°C and checked after 24 h for bacterial colony quantification.

The NBTL agar plates were made by autoclaving nutrient agar (28 g/L) and adding 25 mg/L bromothymol blue and 40 mg/L of triphenyltetrazolium chloride (TTC) before shaking vigorously. Bromothymol blue is a pH indicator and, indirectly, an aerobic indicator. Acid byproducts result in many bacteria producing yellow or red colonies on these plates. *X. nematophila* F1D3 produce deep blue colonies on these plates, presumably because these bacteria do not produce acids by fermentation. For a random sample, the identity of these bacteria was verified using PCR. Following the incubation period at 28°C, the CFUs were counted for each sample, and using the dilution factor at which colonies could be reliably counted, the CFU/ml hemolymph were determined.

Larvae were weighed at the start of the experiment, prior to placement on the chemically defined diet, and then every 24 h up to 96 h (72 h post-challenge). Larvae were also weighed immediately before hemolymph sampling and diet was replaced every 24 h up to 72 h (48 h post-challenge). Ninety-six h after moulting into L6, the larvae had either pupated or were placed on standard semi-artificial diets until death or pupation. All larvae were monitored for death every hour throughout the duration of the sampling period (12 – 36 h) and as frequently as possible thereafter until death or pupation. The date and time of death was recorded, as well as the larval weight at death. None of the weight metrics gathered proved to be significant predictors of mortality risk and so are not discussed further.

Where logistically possible, within an hour of death, hemolymph samples were taken and serially diluted in PBS buffer (pH 7.4) down to 10^{-10} in intervals of 10^{-1}. The dilution series was plated from 10^{-3} to 10^{-10} onto NBTL agar plates (20 μl per 1/4 agar plate). The plates were then incubated at 28°C and checked regularly for CFU, as above.

To try to understand the mechanisms underpinning the main findings, we conducted four additional experiments to explore the relationships between host hemolymph protein, osmolality and bacterial growth rate. In the first experiment, we used synthetic hemolymphs that mimicked the nutritional content of insect blood after feeding on one of twenty diets that varied in their protein and carbohydrate content [34]. For each synthetic hemolymph, 180 uL was placed in each of three wells of a Corning 96-well plate (Sigma-Aldrich), together with 20 uL *X. nematophila* (1×10^7 cells/mL). The plate was then placed into a spectrophotometer (SpectraMax Plus microtiter plate reader with SoftMax Pro software; Molecular Devices) at 28°C for 30 h and bacterial growth rate quantified as maximum absorbance at 600 nm.

In the second experiment, ten newly moulted L6 larvae were reared on each of the six diets for 24 h before a hemolymph sample was taken by piercing larvae with a sterile syringe needle in the anterior pro-leg. Osmolality was measured using an osmometer (Gonotec Osmomat 3000-M, Wolflabs Ltd) after cellular debris was removed by centrifuging the hemolymph at 3000 g for 7 min.

In the third experiment, a range of synthetic hemolymphs were created by combining 10% Grace's Insect Medium (Sigma-Aldrich) with various amounts of KCl (Sigma-Aldrich) and standardized to pH 7.4. The osmolalities of these solutions were again quantified using an osmometer, and 180 uL of each solution was placed in each of three wells of a Corning 96-well plate (Sigma-Aldrich), together with 20 uL *X. nematophila* (1×10^7 cells/mL). The plate was then placed into a spectrophotometer (SpectraMax Plus

Please cite this article in press as: Wilson et al., Osmolality as a Novel Mechanism Explaining Diet Effects on the Outcome of Infection with a Blood Parasite, Current Biology (2020), https://doi.org/10.1016/j.cub.2020.04.058

microtiter plate reader with SoftMax Pro software; Molecular Devices) at 28 C for 30 h and bacterial growth rate quantified as maximum absorbance at 600 nm.

In the final experiment, larvae were fed *ad libitum* for 48h on one of seven diets before being challenged with live *X. nematophila* bacteria (5 μl at 5089 cells/ml PBS) or being sham-injected (PBS only). The seven diets included diets A, C, E and F, as well as three new diets (A3, A6 and A8), which have the same macronutrient composition as diet A, but supplemented with various amounts of a Wesson Salt Mixture (Sigma-Aldrich). These were designed to increase the hemolymph osmolality of the larvae on each diet to that observed on diets C, E and F. After 20 h, all larvae were bled and their hemolymph was diluted in PBS buffer in a tenfold serial dilution (up to 10^6) and plated out on NBTL agar to determine bacterial load, as previously. Data analysis was restricted to those larvae that had an actively replicating bacterial population at the sampling point.

QUANTIFICATION AND STATISTICAL ANALYSIS

All statistical analyses were conducted using the *R* statistical package version 3.5.1 [55]. Ten candidate models were compared (Table 1) using AIC values corrected for finite sample sizes (AIC_c) to establish the most parsimonious models including likely nutritional attributes driving the observed data [56]. AIC_c values and *Akaike weights* were estimated using the *MuMin* package [57]. Both bacteria-challenged and non-challenged larvae were included in the statistical analyses that follow, with bacterial dose included as a $\log_{10}$-transformed covariate with the control insects given a challenge dose of zero. Subsequent analyses indicated that similar qualitative trends are apparent if the control insects are excluded from the analyses. Tables describing the results of the statistical analyses are included in Data S1.

Survivorship

Cox's proportional hazards models were used to establish the effects of diet, bacterial dose ($\log_{10}$-transformed) and their interaction on survivorship post-challenge until death (in the larval, pupal or moth stage), using the *coxph* function in the *survival* package [58]. Nine individuals were excluded from the analysis because their timing of death could not be accurately established, leaving 459 individuals (318 bacteria-challenged and 141 non-challenged control larvae). The predicted values from the model are visualized using thin-plate spline plots created using the *fields* package [59]. These heatmaps depict the risk or odds of dying (relative to 1), such that a risk score above 1 is higher risk and below 1 is lower risk than the population average.

In vivo bacterial growth rate

A subset of larvae were sampled at 12, 16 and 20 h post-challenge to estimate bacterial growth rate, reducing the sample size to 230 larvae (159 bacteria-challenged and 71 non-challenged controls). Inspection of the frequency distribution of bacterial counts revealed that they conformed to a zero-inflated negative binomial model. Therefore, the effects of diet, bacterial dose ($\log_{10}$-transfomed) and their interaction, plus associated covariates (i.e., sample dilution factor, sampling time) were analyzed using the *zeroinfl* function in the *pscl* library [60, 61]. This model provides separate estimates for the negative binomial component (i.e., mostly positive bacterial counts) and the zero-inflated component (zero counts over and above those estimated by the best fit negative binomial distribution).

Bacterial loads at death

For a subset of bacteria-challenged larvae, it was possible to estimate their bacterial load at death. The CFU count multiplied by the serial dilution factor exhibited a negative binomial distribution, and so these data were modeled using the *glm.nb* function in the *MASS* package [62]. Model convergence was possible only when two outliers ($> 10^{10}$ CFU/μl) were excluded from the analysis, giving a sample size of 206 larvae for which the relationships between bacterial dose ($\log_{10}$-transfomed), diet, and bacterial load at death could be established. In a secondary analysis, the relationship between bacterial growth rate (i.e., bacterial load at live sampling) and bacterial load at death was explored, and this reduced the sample size to 126 larvae for which both counts were available.

Correlation between survivorship and bacterial growth rates

In this Cox's proportional hazards model, both bacterial load at sampling (a correlate of *in vivo* bacterial growth rate) and larval diet attributes were included as potential explanatory terms. This allowed us to consider whether larval diet had any effects on survivorship over and above those it may have on bacterial replication rate. The magnitude of challenge dose and time of sampling were also included in the model, as well as the interaction between sampling time and bacterial load at sampling (preliminary analyses indicated that other two-way interactions did not explain a significant amount of variation in survivorship).

Correlation between bacterial growth rates and hemolymph osmolality

The relationship between the amount of protein or carbohydrate in the diet and *in vitro* bacterial growth rate was analyzed using a linear model (LM). The relationship between the amount of protein in the diet and larval hemolymph osmolality was analyzed using a quadratic linear model (LM). The relationship between the osmolality of the synthetic hemolymphs and *in vitro* bacterial growth was analyzed using a generalized additive model (GAM) with Gaussian errors using the *mgcv* package [63]. The relationship between larval hemolymph osmolality and bacterial load *in vivo* was analyzed using a LM with osmolality and diet additive (and their interaction) included as explanatory terms.